19th Australasian Fluid Mechanics Conference
Melbourne, Australia
8-11 December 2014

Simulation of a Transient Supersonic Jet

W. A. Miller[1], C. J. Doolan[1], Z. D. Prime[1], and M. Kim[1]

[1]School of Mechanical Engineering
University of Adelaide, Adelaide, South Australia, 5005 AUSTRALIA

Abstract

This study investigates the evolution of under-expanded jets into a quiescent atmosphere using two-dimensional numerical simulation. The test case consists of two chambers separated by a wall with a small orifice. Initial pressure ratios between the two chambers were varied between 88 and 700, and the jet gas type was high pressure air exhausting into a low pressure, quiescent air chamber. During the initial transient, a Mach shock forms by rapid lateral expansion of the gas near the corner of the orifice and is initially absent at the jet centreline. As the flow evolves, the Mach shock becomes fully formed and vortex rings develop by Kelvin-Helmholtz and baroclinic instabilities at the interface of the barrel shocks and the quiescent air. After further flow evolution, the inner structure of the jet, enclosed by a barrel shock and Mach shock, resembles the structure of a steady under-expanded jet.

Introduction

The control force of a Reaction Control (RC) jet actuator is developed through two primary mechanisms: the thrust of the jet, and the interaction force between the jet and crossflow. Several studies, including Fric and Roshko [9], have characterised the vortical structure of a steady incompressible jet interacting with a crossflow. This structure remains largely unchanged for compressible jets [12]. The shock structure of a steady compressible jet has been investigated by several authors and has been reviewed by Mahesh [12]. These studies have shown that both the shock and turbulent structures of the flow influence the steady interaction force. However, the transient nature of the shock and turbulent structures and their impact on the interaction force between an RC jet and crossflow are not well understood. It has been shown that a jet with linearly increasing thrust in a Mach 3 to 5 crossflow, has a shock structure established within 1 ms, and a wake structure that develops over 4 ms [3]. Further, there is a large overshoot in the control force on jet startup. Ebrahimi [7] showed that these conclusions hold for an instantaneous thrust input, and that the magnitude of the overshoot depends on the jet to crossflow pressure ratio, but the buildup time of the control force does not. DeSpirito [6] found that in a supersonic crossflow, the steady jet force is reached more quickly than in transonic flow, while the transient force overshoot in supersonic flow is much smaller. From this work, it is clear that the shock structure and turbulent structure evolve on different timescales, but their individual contribution to the control force is less clear. Jet outflow conditions, Mach number and pressure ratio all affect the transient interaction. This study is a step toward addressing these issues by isolating the development of shock and vortex structures in a canonical problem, the transient development of a jet into a quiescent atmosphere. This is a critical step in understanding the transient RC jet flowfield.

Naboko and others studied the transient formation of sonic and supersonic jets from a shock tube into a quiescent atmosphere. Results published included initial shock locations and jet gas locations for: sonic argon and nitrogen jets [8]; and supersonic argon, nitrogen and carbon dioxide jets [1, 14]. These studies identified that high pressure jet flow initially forces a strong shock into the atmosphere and that initially, the shock wave structure resembles that of a stationary under-expanded jet. This structure changes with time. The strength of the lead shock diminishes with downstream distance and degenerates into an X-shaped formation before disappearing. Secondary shocks are formed around the orifice due to rapid lateral expansion of the gas. The shape of the secondary shocks changes from almost spherical to virtually flat, eventually weakening and disappearing. It was also reported that vortex rings can be seen to develop at the edge of the nozzle [14]. As the flow forces these vortex structures downstream, they increase in size, decay and the jet becomes turbulent. A schematic showing each of the flow structures is provided in figure 1, which has been adapted from [15].

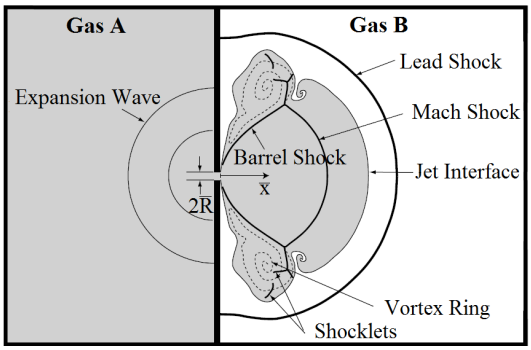

Figure 1. Schematic showing jet structures, adapted from [15].

The development of vortex rings in a jet flow was also studied by Gharib, Rambod and Shariff [10], who showed that, for jet injections with a short pulse, almost all the jet fluid is entrained within a starting vortex, which is generated via separation of the boundary layer at the edge of the orifice. However, for jet injections with a longer pulse, the starting vortex reaches a limiting size. Beyond this size, vorticity remains in the shear layer and is not entrained in the starting vortex. Two-dimensional, inviscid simulations of a hydrogen jet into quiescent air were performed by Raduelscu and Law [15], with pressure ratios between 100 and 1000. Radulescu and Law described the initial development of the shock structure, the establishment of a regime that appears dynamically similar, and later stages of flow evolution. Kelvin-Helmholtz and baroclinic instability were identified as mechanisms for vorticity generation, while Rayleigh-Taylor instabilities were found to be present in the flow interface when $\tilde{\rho_{Ai}}/\tilde{\rho_{Bi}} > 1$, where tilda denotes a solution of the one-dimensional shock tube problem [15]. For hydrogen in air, this corresponds to a pressure ratio of 337.

This paper presents the numerical simulation of two-dimensional transient supersonic jets into a quiescent atmosphere. The numerical setup will be described, followed by the simulation results. Results include justification of grid independence and associated error estimation, validation of the model, and description of the turbulent and shock structures. Finally, conclusions and proposals for future work will be presented.

Numerical Setup

OpenFOAM^{TM} has been used to simulate the flow of air jets into still air. Since we are interested in high Reynolds number jets, it is assumed that convective fluxes will dominate over diffusive fluxes in the majority of the flowfield and therefore the flow can be considered inviscid. It is also assumed that the flow is in chemical equilibrium and the air behaves as a perfect gas, with $\gamma = 1.4$. The physical setup of the simulations replicates [15] and is shown in the schematic in figure 1. High pressure gas (gas A) is initially separated from a low pressure gas (gas B), with both gases at rest. At the beginning of the simulation, gas A is allowed to flow freely into gas B through an orifice of radius $\overline{R}$ at $\overline{x} = 0$. In this paper, we will adopt the convention of [15], where an overbar indicates a dimensional quantity and, generally, results will be presented in non-dimensional co-ordinates, defined as follows:

$$x \equiv \frac{\overline{x}}{\overline{R}}; u_i \equiv \frac{\overline{u_i}}{\overline{a}_{Ac}}; \rho \equiv \frac{\overline{\rho}}{\overline{\rho}_{Ac}}; p \equiv \frac{\overline{p}}{\overline{\rho}_{Ac}\overline{a}^2_{Ac}} = \frac{\overline{p}}{\gamma_A \overline{p}_{Ac}}; t \equiv \frac{\overline{t}\overline{a}_{Ac}}{\overline{R}} \tag{1}$$

$\overline{a}_{Ac}$ and $\overline{\rho}_{Ac}$ are calculated for a steady isentropic expansion from the stagnation state of gas A as follows [15]:

$$\overline{a}_{Ac} = \overline{a}_{Ao}\left(\frac{2}{\gamma_A + 1}\right)^{\frac{1}{2}}; \overline{\rho}_{Ac} = \overline{\rho}_{Ao}\left(\frac{2}{\gamma_A + 1}\right)^{\frac{1}{(\gamma_A - 1)}} \tag{2}$$

Subscripts c and o refer to the choked and stagnation states respectively. The computational domain consists only of the upper half of the flow, with an axis of symmetry applied at the jet centreline ($y = 0$). The domain includes chambers of both gases A and B with adiabatic walls sufficiently far away that shocks are not reflected. Gases A and B are separated by an adiabatic wall of thickness 0.125. All simulations have been conducted to second order accuracy using the OpenFOAM^{TM} solver *rhoCentralFoam*, a density-based, compressible flow solver that uses central schemes proposed by Kurganov and Tadmor [11]. Table 1 gives the initial conditions for gases A and B in each simulation.

Case	p_{Ao}/p_{Bo}	ρ_{Ao}/ρ_{Bo}	T_A/T_B
1	88.0	6.1	1.0
2	337	23	1.0
3	700	48	1.0

Table 1. Initial conditions for gases A and B in each simulation.

Results

Grid Independence Study

To check for grid independence, simulations were conducted on three grids (100×210 cells, 200×425 cells and 400×850 cells). All three grids are structured in the jet region, with a buffer of unstructured mesh before the domain walls to ensure no waves are reflected. Figure 2 (a) shows the estimated values of peak temperature for Case 1 at the location x = 10, y = 0.5, plotted against a representative cell size measure, Δ, i.e. $\Delta = \sqrt{1/N_{cells}}$ as defined by [4]. Also shown in figure 2 (a) is a line fitted through the three points that follows:

$$f(\Delta) = f_{limit} - C\Delta^p \tag{3}$$

where $f(\Delta)$ is the flow parameter of interest estimated on the grid characterised by Δ, f_{limit} is the limiting value of the flow

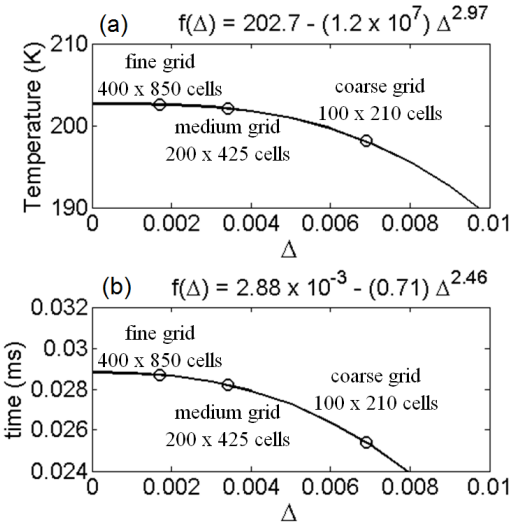

Figure 2. (a) Peak temperature for Case 1 at x = 10, y = 0.5, and (b) Time taken for lead shock to reach x = 10, y = 0.5 in Case 1.

parameter for infinite grid resolution, C is a constant, and p is the order of convergence [4]. Figure 2 (a) shows that, for about third order convergence, the limiting value of peak temperature is 202.7 K. This gives 0.03 %, 0.28 % and 2.26 % errors for the three grids. Similarly, figure 2 (b) shows the time taken for the lead shock to reach x = 10, y = 0.5 in Case 1. For second order convergence, the limiting value of time is 0.0288 ms and the errors on the fine, medium and coarse grids are 0.3 %, 2.1 % and 11.8 % respectively. The medium grid (200×425 cells) provides acceptable accuracy, however, as noted by Radulescu and Law [15], a solution to the flow with large density gradients and regions of high vorticity using the inviscid Euler equations is not truly independent of the chosen grid resolution. The small scales of the barrel shock and vortex ring can only converge if the dissipation is correctly modelled. Nevertheless, the simulations are able to capture development and motion of the shocks and vortex regions and show second order convergence. The remainder of this paper will focus on the medium (200×425 cells) grid.

Model Validation

The evolution of the flowfield was captured by Naboko et al. via schlieren photography [13], and is compared qualitatively to the simulation results in figure 3. Major shock structures, including lead shock, Mach shock and barrel shock, are captured by the simulation. The relative speed of shock and jet gas propagation differs, owing to the different jet gases, as expected. The vortex ring has also been captured. Quantitative validation is performed by comparison of shock and fluid interface locations to several authors via a database compiled by Radulescu and Law, consisting of experimental, numerical and analytical results [15]. Figure 4 shows the shock and interface locations, in non-dimensionalised co-ordinates, defined as follows [15]:

$$\varepsilon \equiv \rho_{Bo}{}^{\frac{1}{j}} \frac{x}{\Lambda}; \tau \equiv \rho_{Bo}{}^{\frac{1}{j}} \frac{t}{\Lambda} \tag{4}$$

where ρ_{Bo} is the initial density of gas B, j is the geometric index (j = 1 for axial symmetry) , and Λ is the non-dimensional radius of the choked source ($\Lambda = 1$ for a slit jet).

Excellent agreement is obtained between the current model and previous experimental data, indicating that the simulation does indeed predict the correct shock and interface velocity. The con-

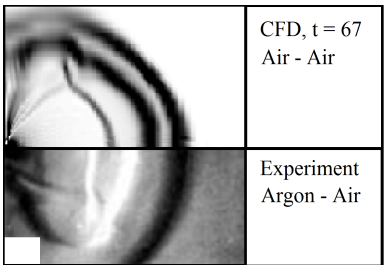

Figure 3. Comparison of transient jet development for Case 2 with experiment ([13] adapted from [15]).

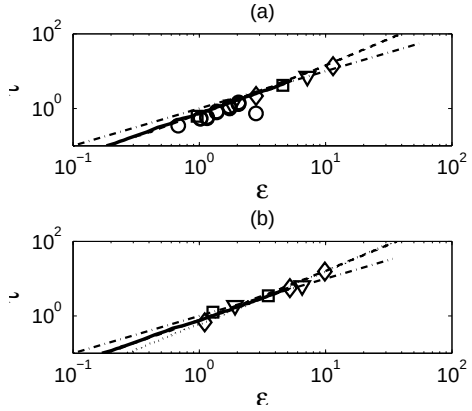

Figure 4. Comparison of the predicted (a) shock, and (b) interface location with experimental, numerical and analytical data. Solid line: Case 2 prediction Air - Air; dot-dash line: Radulescu & Law (2007) [15] H_2 - Air; dash line: Radulescu & Law (2007) [15] model; dotted line: Chekmarev & Stankus (1984) [5] model; ○: Buckmaster (1964) Air - Air [2]; ▽: Belavin et al. (1973) $N_2 - N_2$ [1]; □: Belavin et al. (1973) $CO_2 - CO_2$ [1]; and ◇: Belavin et al. (1973) Ar - Ar [1].

clusion can be drawn that the simulations correctly represent the flowfield and predict the motion and evolution of both the shocks and the jet fluid, with acceptable error.

Flowfield

The early stages of flow development are described in figure 5 in terms of pressure gradient. The lead shock forms immediately and is normal to the flow through the orifice, before being curved by the lateral jet expansion at the edge of the orifice. Following this initial phase, the lead shock develops and maintains an almost circular shape and reduces in strength as the flowfield evolves. As predicted by experiment [14], the strength of the Mach shock also diminishes with downstream distance. However, the formation of the shock structure is more complex than that reported by Naboko et al. The Mach shock and barrel shock form by lateral expansion of the jet gas around the orifice corner. As such, the Mach shock is not initially present at the jet axis. A one-dimensional expansion centred at x = 0 is also formed, along with additional expansion and compression waves that form due to lateral expansion of the flow. The lateral expansion wave reflects and is amplified behind the Mach shock by negative pressure and density gradients to form an additional shock, which traverses the Mach and barrel shocks. This shock structure is in agreement with the structure of a hydrogen jet reported in [15]. The corresponding vorticity fields are shown in figure 6 at the same times as the shock structure in figure 5. Initially, vorticity forms at the jet orifice and is entrained into both the lead shock and the Mach shock as well as the starting vortex. As the flow evolves, vorticity continues to be produced at the corner of the orifice, forming a vortex structure that closely replicates the long jet pulse described in [10]. Shocklets form in the shear layer and vortex ring. The flow structure in this region is under-resolved in this simulation, but similar features have been reported in [15]. Further investigation of this region requires a viscous simulation, so grid refinement in this area was not required for this work.

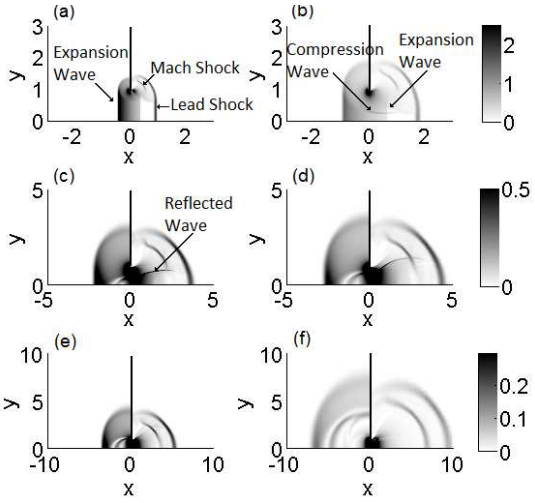

Figure 5. Contours of non-dimensional pressure gradient showing development of shock structure for Case 2 at (a) t = 0.5, (b) t = 1, (c) t = 2, (d) t = 2.5, (e) t = 3.2, (f) t = 6.3.

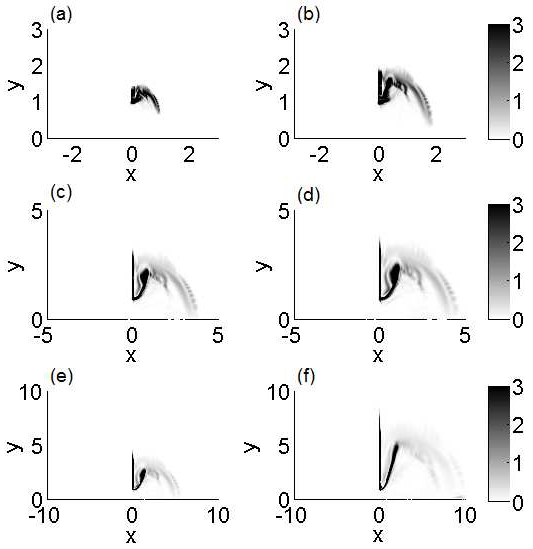

Figure 6. Contours of non-dimensional vorticity magnitude showing development of turbulent structure for Case 2 at (a) t = 0.5, (b) t = 1, (c) t = 2, (d) t = 2.5,(e) t = 3.2, (f) t = 6.3.

Figure 7 shows the evolution of the pressure and velocity fields along the symmetry axis. At t = 1, the flow along the jet axis is analogous to a one-dimensional expansion. At later times, the effects of lateral expansion can be seen and the throat begins to form. The pressure drops faster than can be accommodated by the lead shock decay and the compression wave is amplified to form an additional shock, as described previously.

After t = 15, the Mach shock evolves to join at the jet centreline and the barrel shock remains attached to the corner of the orifice, and grows in length as the Mach shock moves downstream

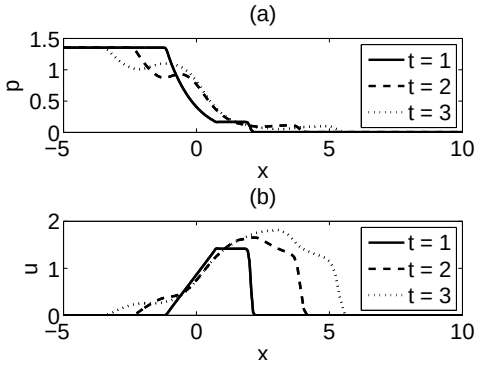

Figure 7. (a) Pressure and (b) Velocity profiles along axis of symmetry (y = 0) for Case 2 at t = 1, t = 2, and t = 3.

with the fluid interface. As shown in figure 8, this forms the well known steady jet shock and turbulence structure referred to as the dynamically similar regime in [15]. This transition to a dynamically similar regime occurs much later than reported in [15], due to differences between hydrogen and air jets. The corresponding vorticity field seems to evolve over the same time scale to appear dynamically similar after t = 15. However, this prediction is tentative, as a viscous simulation and a tighter grid are required to resolve and predict the vortex ring.

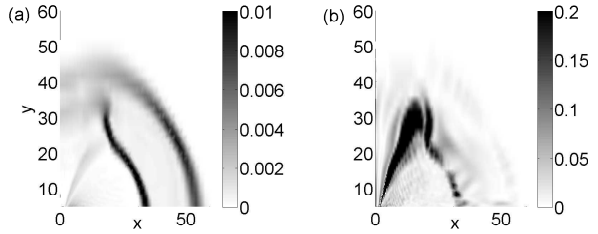

Figure 8. Contours of (a) non-dimensional pressure gradient, and (b) non-dimensional vorticity magnitude showing fully developed shock and turbulent structures for Case 2 at t = 50.

Conclusions and Future Work

This work has investigated the development of shock and turbulent structures of an air jet in a quiescent air atmosphere via two-dimensional, inviscid simulations. The results compared very well with previous studies. The structure of shocks, expansion and compression waves is initially complex, and consists of: an almost circular lead shock; a partial Mach shock; a barrel shock; a one-dimensional expansion wave; and additional expansion and compression waves formed by lateral expansion. Vorticity is initially developed at the corner of the orifice and spreads within the lead and Mach shocks. At later times ($t > 15$) the dynamically similar regime is formed and vorticity continues to form at the orifice corner, but remains entrained within the shear region and vortex ring. Evolution of the flow to reach a dynamically similar regime takes the same amount of time for both the shock and vortex structures.

This work has shown the ability of OpenFOAM^{TM} to simulate a jet flow and has confirmed the jet structure described by Radulescu and Law [15] for a hydrogen jet also applies to air jets. However, development of air jets to a dynamically similar regime takes longer. Future work will be to conduct viscous simulations and investigate the impact this has on the vorticity of the flow. Once the flowfield of a jet in quiescent atmosphere is known, the influence of a crossflow will also be investigated, to finally identify the influence of the shock and turbulent structures on the RC jet transient control force.

References

[1] Belavin, V. A., Golub, V. V., Naboko, I. M. and Opara, A. M., Study of the structure of a time-dependent flow created by an emerging stream of shock-heated gas., *Journal of Applied Mechanics and Technical Physics*, **5**, 1973, 34 – 40.

[2] Buckmaster, J. D., An investigation of cylindrical starting flows, *AIAA Journal*, **2**, 1964, 1649 – 1650.

[3] Chamberlain, R., McClure, D. and Dang, A., CFD Analysis of Lateral Jet Interaction Phenomena for the THAAD Interceptor, in *AIAA Aerospace Sciences Meeting and Exhibit, Reno, NV*, 2000.

[4] Chan, W. Y. K., Jacobs, P. A. and Mee, D. J., Suitability of the $k-\omega$ turbulence model for scramjet flowfield simulations, *International Journal for Numerical Methods in Fluids*, **70**, 2012, 493 – 514.

[5] Chekmarev, S. F. and Stankus, N. V., Gasdynamic model and similarity relations for the starting process in supersonic nozzles and jets, *Soviet Physics - Technical Physics*, **29**, 1984, 920 – 925.

[6] DeSpirito, J., Transient Lateral Jet Interaction Effects on a Generic Fin-Stabilized Projectile, in *AIAA Applied Aerodynamics Conference, New Orleans, LA*, 2012.

[7] Ebrahimi, H. B., Numerical Simulation of Transient Jet-Interaction Phenomenology in a Supersonic Freestream, *AIAA Journal of Spacecraft and Rockets*, **37**, 2000, 713 – 719.

[8] Eremin, A. V., Kochnev, V. A., Kulikovskii, A. A. and Naboko, I. M., Nonstationary Processes in Starting Strongly Underexpanded Jets, *Journal of Applied Mechanics and Technical Physics*, **19**, 1978, 27 – 31.

[9] Fric, T. F. and Roshko, A., Vortical structure in the wake of a transverse jet, *Journal of Fluid Mechanics*, **279**, 1994, 1 – 47.

[10] Gharib, M., Rambod, E. and Shariff, K., A universal time scale for vortex ring formation, *Journal of Fluid Mechanics*, **360**, 1998, 121 – 140.

[11] Kurganov, A. and Tadmor, E., New High-Resolution Central Schemes for Nonlinear Conservation Laws and Convection-Diffusion Equations, *Journal of Computational Physics*, **160**, 2000, 241 – 282.

[12] Mahesh, K., The Interaction of Jets with Crossflow, *Annual Review of Fluid Mechanics*, **45**, 2013, 379 – 407.

[13] Naboko, I. M., Bazhenova, T. V., Opara, A. I. and Belavin, V. A., Formation of a jet of shock-heated gas outflowing into evacuated space, *Acta Astronautica*, **17**, 1972, 653 – 658.

[14] Naboko, I. M., Belavin, V. A. and Golub, V. V., Nonstationary wave structure of intermittent supersonic jet, *Acta Astronautica*, **6**, 1979, 885 – 899.

[15] Radulescu, M. I. and Law, C. K., The transient start of supersonic jets, *Journal of Fluid Mechanics*, **578**, 2007, 331 – 369.